



HAL
open science

Pharmacological differentiation of opioid receptor antagonists by molecular and functional imaging of target occupancy and food reward-related brain activation in humans

Edward Bullmore, Eugenii Rabiner, John Beaver, Aidan Makwana, Graham Searle, Christopher Long, Pradeep Nathan, Rexford Newbould, Jonathan Howard, Sam Miller, et al.

► To cite this version:

Edward Bullmore, Eugenii Rabiner, John Beaver, Aidan Makwana, Graham Searle, et al.. Pharmacological differentiation of opioid receptor antagonists by molecular and functional imaging of target occupancy and food reward-related brain activation in humans. *Molecular Psychiatry*, 2011, 10.1038/mp.2011.29 . hal-00633601

HAL Id: hal-00633601

<https://hal.science/hal-00633601>

Submitted on 19 Oct 2011

HAL is a multi-disciplinary open access archive for the deposit and dissemination of scientific research documents, whether they are published or not. The documents may come from teaching and research institutions in France or abroad, or from public or private research centers.

L'archive ouverte pluridisciplinaire **HAL**, est destinée au dépôt et à la diffusion de documents scientifiques de niveau recherche, publiés ou non, émanant des établissements d'enseignement et de recherche français ou étrangers, des laboratoires publics ou privés.

Pharmacological differentiation of opioid receptor antagonists by molecular and functional imaging of target occupancy and food reward-related brain activation in humans

Eugenii A. Rabiner, FCPsych SA^{1,2}¶, John Beaver, PhD¹¶, Aidan Makwana MEng¹, Graham Searle PhD¹, Christopher Long PhD¹, Pradeep J. Nathan, PhD^{3,4}, Rexford D. Newbould PhD¹, Jonathan Howard PhD¹, Sam R. Miller MSc⁵, Mark A. Bush PhD⁶, Samuel Hill BSc¹, Richard Reiley BA¹, Jan Passchier PhD¹, Roger N. Gunn PhD^{1,2,7}, Paul M. Matthews, DPhil^{1,2}, Edward T. Bullmore, PhD^{3,4,*}

- 1) GSK Clinical Imaging Centre, Imperial College London, Hammersmith Hospital, Du Cane Road, London W12 0NN, UK
- 2) Centre for Neurosciences, Division of Experimental Medicine and Toxicology, Imperial College, London W12 0NN, UK
- 3) GSK Academic Discovery Performance Unit and Clinical Unit Cambridge, Addenbrooke's Centre for Clinical Investigations, Cambridge Biomedical Campus, Cambridge CB2 0GG, UK
- 4) Behavioural & Clinical Neuroscience Institute, Department of Psychiatry, University of Cambridge, CB2 0SZ, UK
- 5) GSK Quantitative Sciences, Gunnels Wood Road, Stevenage, SG1 2NY, UK
- 6) GSK Clinical Pharmacology Modeling and Simulation, 5 Moore Drive, Research Triangle Park, NC 27709, USA
- 7) Department of Engineering Science, University of Oxford, Oxford, UK

¶ These authors contributed to this manuscript equally

* **Correspondence:** Professor Ed Bullmore, Academic DPU, Addenbrooke's Centre for Clinical Investigations, Cambridge Biomedical Campus, Cambridge CB2 0GG, UK. Tel: +44 (0)1223 296100. Fax: +44 (0)1223 296108. Email: edward.t.bullmore@gsk.com

Disclosure: The study was sponsored by GlaxoSmithKline (<http://www.gsk.com>) and the protocol was posted on <http://clinicaltrials.gov> (NCT00976066) prior to study initiation. Appropriate ethical committee and regulatory approvals were obtained from the NHS Brent Medical Ethics Committee, Northwick Park Hospital, Middlesex, UK (Ref. 09/H0717/30), the Medicines & Healthcare products Regulatory Agency (MHRA Clinical Trial Authorization; EudraCT number 2009-010358), and the Administration of Radioactive Substances Advisory Committee, UK Health Protection Agency (ARSAC number RPC 612/3764/24660). All PET and MRI scans were conducted at the GSK Clinical Imaging Centre, Hammersmith Hospital, London, UK. Overnight stays and non-scanning procedures were carried out by Hammersmith Medicines Research, Park Royal, London, UK. Venous plasma samples were analysed at the GlaxoSmithKline Drug Metabolism and Pharmacokinetics laboratories in Ware, UK (for GSK1521498) and in Durham, NC, USA (for naltrexone and 6- β -naltrexol).

Word count: 3489 plus 230 in Abstract, 4 Figures, 1 Table, Supplementary Information

ABSTRACT

Opioid neurotransmission plays a key role in mediating reward-related behaviours. Opioid receptor antagonists such as naltrexone (NTX) can attenuate the behaviour-reinforcing effects of primary (food) and secondary rewards. GSK1521498 is a novel opioid receptor (OR) ligand, which behaves as an inverse agonist at the μ -OR subtype. In a sample of healthy volunteers, we used [^{11}C]-carfentanil PET to measure opioid receptor occupancy and functional MRI to measure activation of brain reward centres by palatable food stimuli before and after single oral doses of GSK1521498 (range, 0.4-100mg) or NTX (range, 2-50 mg). GSK1521498 had high affinity for human brain opioid receptors (GSK1521498 $\text{EC}_{50} = 7.10 \text{ ng/ml}$) and there was a direct relationship between receptor occupancy (RO) and plasma concentrations of GSK1521498. However, for both NTX and its principal active metabolite in humans, 6- β -naltrexol (6- β -NTX), this relationship was indirect. GSK1521498, but not NTX, significantly attenuated the fMRI activation of the amygdala by a palatable food stimulus. We thus have shown how the pharmacological properties of opioid receptor antagonists can be characterised directly in humans by a novel integration of molecular and functional neuroimaging techniques. GSK1521498 was differentiated from NTX in terms of its pharmacokinetics, target affinity, plasma concentration-receptor occupancy relationships, and pharmacodynamic effects on food reward processing in the brain. Pharmacological differentiation of these molecules suggests that they may have different therapeutic profiles for treatment of over-eating and other disorders of compulsive consumption.

Keywords: positron emission tomography, functional MRI, experimental medicine, pharmacokinetics, pharmacodynamics, neuropharmacology

INTRODUCTION

The endogenous opioid neurotransmitter system comprises a number of peptides (including β -endorphins, enkephalins and dynorphins) and three major opioid receptor (OR) sub-types: μ , δ and κ ¹⁻³. Opioid receptor agonists increase, whereas antagonists decrease, feeding and other rewarding behaviours in animal models⁴⁻⁹. Agonism at the μ -OR subtype appears to be particularly effective in enhancing hedonic and consummatory eating behaviours^{6, 10-12}, as demonstrated by greater intake of energy-dense foods. This effect is blocked by opioid receptor antagonists^{13, 14}. Direct infusion of μ -OR agonists has been used to localise effects on eating behaviour to the nucleus accumbens in rats^{10-13, 15, 16}. The basal nucleus of the amygdala provides a major input to the nucleus accumbens¹⁷, amplifying the hedonic value of palatable food and its motivational influence on goal-directed behaviours^{18, 19, 20, 21, 22}.

Opioid signalling in humans has been implicated in behaviours reinforced by primary rewards, especially fatty or sugary foods, or secondary rewards, such as self-administered drugs. Acute administration of drugs broadly classified as OR antagonists (e.g., naltrexone [NTX]) moderately reduces short-term food intake²³ and affective or subjective pleasantness of palatable foods in healthy subjects²³⁻²⁶; and reduces food or drug intake in short-term animal and experimental medicine models of obesity, binge-eating, alcohol and drug dependence syndromes²³⁻²⁸. NTX is licensed for treatment of alcohol and opiate addiction.

GSK1521498 is a novel opioid receptor ligand with a high degree of selectivity for the μ -OR subtype in binding studies (**Table 1**). It has antagonist effects at the μ -OR receptor, or inverse agonist properties under conditions of constitutive receptor activity. In a first-in-human (FTIH) acute dose escalation study, single doses were safe and well tolerated up to a

maximum tolerated dose of 100mg²⁹. A single 25mg dose of GSK1521498 was associated with reduced pleasurable response to, and reduced consumption of, high fat/high sugar snack items in an experimental model of over-eating behaviour in overweight volunteers²⁹.

Here, we used neuroimaging to investigate μ -OR occupancy and effects on brain function of single doses of naltrexone and GSK1521498 in healthy volunteers. We used positron emission tomography (PET) with [¹¹C]-carfentanil to measure μ -OR occupancy over a range of doses and plasma concentrations of both drugs. In the same scanning sessions, we also used functional magnetic resonance imaging (fMRI) to measure food reward-related activation of theoretically predicted brain regions, including amygdala and striatum³⁰⁻³⁵. We compared the two drugs in terms of their pharmacokinetics, target occupancy, and proximal functional efficacy.

MATERIALS and METHODS

Participants

Twenty-six healthy male volunteers (25-60 years old, body weight > 50 kg and body mass index (BMI) 19-30 kg/m²) were recruited from the London area by a research organization, Hammersmith Medical Research, contracted by the GSK Clinical Imaging Centre, London. All subjects satisfied eligibility criteria and passed a medical screen for fitness to participate (see **Supplementary Information** (SI) for details), and provided informed consent for participation in writing.

Study design

This was an open label study, with participants assigned to either GSK1521498 or NTX treatment groups at enrollment. Each participant underwent up to three [¹¹C]-carfentanil PET scans and two fMRI examinations: one [¹¹C]-carfentanil PET scan and one fMRI scan at baseline (before dosing) and up to two PET scans and one fMRI scan following oral administration of a single dose of GSK1521498 or NTX. Two participants opted to withdraw from the study following completion of the baseline scanning session: the complete PET dataset available for analysis therefore comprised 24 participants.

The administered doses of GSK1521498 or NTX were chosen adaptively to optimize the estimation of the dose-occupancy relationship for each drug on the basis of data acquired from the preceding examinations in the study⁴⁴. The administered dose range was 0.4-100mg for GSK1521498, and 2-50mg for NTX. The maximum doses administered were equal to the maximum tolerated dose of GSK1521498 determined in the FTIH study²⁹ and the standard clinical dose of NTX used for alcohol dependence³⁶.

The times and doses of the two post-dose [¹¹C]-carfentanil PET scans were chosen adaptively for each subject to optimise estimation of the relationship between plasma concentration and receptor occupancy (RO)⁴⁴. Post-dose [¹¹C]-carfentanil PET scans were acquired 3-36 h after the administration of GSK1521498 and 3-88 h after the administration of NTX. Post-dose fMRI scans were acquired within 60 mins of the first post-dose PET scan.

Sampling and analysis of drug plasma concentrations

Venous blood samples were collected at regular intervals throughout the scanning sessions. High performance liquid chromatography/mass spectrometry/mass spectrometry (HPLC-MS/MS) was employed to estimate the plasma concentrations of GSK1521498, NTX, and the major metabolite of NTX, 6-β-naltrexol (6-β-NTX) (see **SI** for assay details). Drug plasma concentration at the start of each PET scan was used to model the relationship between drug concentrations and μ-OR occupancies.

[¹¹C]-carfentanil PET data acquisition and pre-processing

Carfentanil (methyl 1-(2-phenylethyl)-4-[phenyl(propanoyl)amino]-4-piperidinecarboxylate 3S, 5S; Advanced Biochemical Compounds, Radeberg, Germany), a potent selective μ-OR agonist, was labelled with carbon-11 using a modification of a previously described method³⁷ implemented using a semi-automated Modular Lab Multifunctional Synthetic Module (Eckert & Ziegler, Germany). The final product was reformulated in sterile 0.9% saline containing approximately 10% ethanol (v/v) and satisfied quality control criteria for specific activity and purity before being injected intravenously as a slow bolus over approximately 30 s.

PET scanning was conducted in 3D mode using a Siemens Biograph 6 Hi-Rez PET-CT for the NTX group and a Siemens Biograph 6 TruePoint PET-CT for the GSK1521498 group (Siemens Healthcare, Erlangen, Germany). A low-dose CT scan was acquired for attenuation correction prior to the administration of the radiotracer. Dynamic PET data were acquired for 90 mins after [¹¹C]-carfentanil injection, binned into 26 frames (durations: 8 × 15 s, 3 × 60 s, 5 × 2 mins, 5 × 5 mins, 5 × 10 mins), reconstructed using Fourier re-binning and a 2D filtered back projection algorithm and then smoothed with a 2D Gaussian filter (5 mm at full width half maximum).

PET data analysis

Dynamic PET images were registered to each participant's T1-weighted anatomical MRI volume and corrected for head motion using SPM5 software (Wellcome Trust Centre for Neuroimaging, <http://www.fil.ion.ucl.ac.uk/spm>). Pre-selected regions of interest (ROIs; amygdala, caudate, putamen, thalamus, cerebellum, frontal and occipital cortices) were defined bilaterally on the T1-weighted anatomical volume using an in-house atlas³⁸ and applied to the dynamic PET data to generate regional time-activity curves (TACs) (**Figure 1**).

[¹¹C]-carfentanil specific binding was quantified as binding potential relative to the non-displaceable compartment (BP_{ND} ³⁹)

$$BP_{ND} = \frac{f_{ND}B_{avail}}{K_D} \quad \text{Eq 1}$$

where f_{ND} is the free fraction of the radioligand in the brain, K_d is the affinity of [¹¹C]-carfentanil, and B_{avail} is the density of the available μ -opioid receptors. Regional [¹¹C]-

carfentanil BP_{ND} was estimated using a reference tissue model⁴⁰ with the occipital cortex as the reference region. Drug related occupancy of the μ -OR was quantified as a reduction of [¹¹C]-carfentanil BP_{ND}

$$Occupancy_{Drug} = \frac{BP_{ND}^{Baseline} - BP_{ND}^{Drug}}{BP_{ND}^{Baseline}} \quad \text{Eq 2}$$

The affinity constant for each drug at the μ -OR (EC_{50}) was estimated by fitting the plasma concentration measured at the start of the PET scan, C_{Drug}^P , to the estimated occupancy:

$$Occupancy_{Drug} = \frac{C_{Drug}^P}{C_{Drug}^P + EC_{50}} \quad \text{Eq 3}$$

Functional MRI: food stimuli and activation paradigm

Food stimuli for the fMRI task were delivered orally in the scanner and, for different trials, were either 0.5 ml of a highly palatable commercially available drink (marketed in the UK as a “smoothie”), 0.5 ml of a neutral solution (25mM KCL and 2.5mM NaHCO₃ in water), or 1.0 ml of purified water. Although data from trials with the neutral solution will not be reported here, the full activation paradigm consisted of 16 palatable drink and 16 neutral solution trials, presented in randomised order. Purified water was delivered after each stimulus trial; we allowed a slightly greater volume of purified water (1 ml) to wash away residual traces of the flavored stimuli (0.5 ml) between trials. To minimise head movements during delivery of the stimuli, participants were instructed to refrain from swallowing until a cue was presented 5 s later.

Functional MRI: data acquisition

T2*-weighted, dual echo, echo-planar images sensitive to blood oxygenation level-dependent (BOLD) contrast were acquired continuously on a 3T Siemens Tim Trio scanner with a 32-channel head coil (Siemens Healthcare, Erlangen, Germany). Each scan session consisted of 390 volumes of a 38-slice acquisition, angled $\sim 30^\circ$ coronally to the anterior-posterior commissural plane to minimise signal dropout in orbitofrontal and medial temporal regions (TR = 2100 ms; dual TEs = 13 and 31 ms; flip angle = 80° , matrix size = 64×64 , and field of view = 225×225 mm for voxel size of $3.0 \times 3.0 \times 3.0$ mm). High-resolution T1-weighted anatomical scans (ADNI MPRAGE⁴¹) were acquired with whole-brain coverage (208 slices) for each participant to facilitate fMRI and PET image co-registration and PET ROI definition (TR = 3000 ms, TE = 3.66 ms, flip angle = 9° , voxel size = 1 mm^3).

Functional MRI: data analysis

Functional MRI data were corrected for head motion, high-pass filtered and spatially smoothed using FSL software: <http://www.fmrib.ox.ac.uk/fsl> (see SI for details). We estimated the difference in regional mean BOLD signal intensity between periods of palatable stimulus delivery and periods of purified water delivery, at each of nine ROIs bilaterally (as defined *a priori* in the protocol at <http://clinicaltrials.gov>). These estimates were then averaged over right and left homologous regions of amygdala, caudate, globus pallidus, hippocampus, insula, nucleus accumbens, orbitofrontal cortex, thalamus and putamen. In each treatment group, we tested the null hypothesis that the within-subject difference between baseline (pre-dose) and post-dose scans in regional BOLD response to palatable stimuli vs purified water was zero: [post-dose BOLD response to palatable trials] – [pre-dose BOLD response to palatable trials] = Δ -BOLD = 0. To control for between-subject variability in μ -

OR occupancy (by either drug) and for variability in BOLD activation at baseline, we also tested Δ -BOLD in each ROI using a linear model including baseline BOLD activation and RO as covariates. To control for multiple comparisons in these planned regional analyses of treatment-related differences in brain activation, the threshold for significance was Bonferroni corrected at $P < 0.05/9 = 0.0055$. We also tested the null hypothesis that there is no difference in Δ -BOLD between drugs ($\Delta\text{-BOLD}_{\text{GSK1521498}} = \Delta\text{-BOLD}_{\text{NTX}}$), and between-drug comparisons were controlled for baseline activation and RO.

We also conducted exploratory voxel-level analyses of the fMRI data. Combining data from both treatment groups, we used the general linear model to estimate activation by palatable stimuli vs. purified water. This contrast was tested by permutation at the level of spatially contiguous supra-threshold voxel clusters, controlling the family-wise probability of type 1 error at $P < 0.05$ to generate a map of the brain systems activated by food reward. Within this reward system, we separately tested at each voxel the hypotheses that $\Delta\text{-BOLD} = 0$ for GSK1521498 and for NTX, and that $\Delta\text{-BOLD}_{\text{GSK1521498}} = \Delta\text{-BOLD}_{\text{NTX}}$. These exploratory whole brain analyses are reported at a cluster-wise level of type I error $P < 0.05$, uncorrected for multiple comparisons.

RESULTS

Evaluable data and samples

PET data used in the analysis consisted of 24 baseline (pre-dose) scans (13 for the GSK1521498 group and 11 for the NTX group) and 44 post-dose scans (24 following GSK1521498 and 20 following NTX). Evaluable fMRI data from 17 participants (9 scanned following GSK1521498 and 8 scanned following NTX) were included in the analysis. The treatment groups of participants with evaluable PET or fMRI data were well matched in terms of: age, BMI, scores on the TFEQ-R18⁴² and BIS-11⁴³ questionnaires of eating behaviour and impulsivity, the self-rated “liking” of their preferred palatable drink stimulus at baseline, dose of radioactivity and injected mass of carfentanil during the PET scans (**SI Table S1**). Neither treatment group demonstrated a significant post-dose reduction in the “liking” score for the palatable food stimuli (**SI Table S1**).

Pharmacokinetics

Plasma exposure parameters are summarised in **Table 1** for GSK1521498, NTX and 6- β -NTX. Representative concentration-time profiles for GSK1521498, NTX and 6- β -NTX administered in the current study are shown in **SI Figure S1**.

[¹¹C]-carfentanil PET data

At baseline, [¹¹C]-carfentanil showed high binding in the striatum, the thalamus and the amygdala (**Figure 1**). Dose dependent reductions in regional BP_{ND} were observed following the administration of both GSK1521498 and NTX in all ROIs except the occipital cortex, justifying its selection as a reference region (**Figure 1**).

There were no regional differences in RO for either drug, so regional occupancies were averaged to estimate global RO. Equation 3 provided a good fit to the data on plasma concentration and RO acquired at all times following a dose of GSK1521498, indicating a direct relationship between exposure and occupancy^{44, 45} (**Figure 2**). We were thus able to estimate the plasma concentration of GSK1521498 associated with 50% occupancy of the μ -OR: $EC_{50} = 7.10$ ng/ml (95% CI= 5.96-8.25 ng/ml). For NTX and 6- β -NTX there was a time-dependent effect (hysteresis) on the exposure-occupancy relationship, i.e., a given plasma concentration resulted in greater occupancy at later time points. Hence, the direct model did not provide adequate characterisation of RO based on plasma concentrations of NTX or 6- β -NTX (**Figure 2**) and time-independent EC_{50} estimates could not be determined for either species.

Due to the dependence of the NTX dose-occupancy relationship on the time post-dose, the dose-occupancy relationships for NTX and GSK1521498 were estimated using data acquired <8 h post-dose. The dose required to achieve 50% RO (ED_{50}) was estimated at 1.50 mg (95% CI = 1.24 – 1.76 mg) for GSK1521498. The apparent ED_{50} for NTX was 5.60 mg (95% CI = 3.65 – 7.54 mg) (**Figure 1**).

Functional MRI data:

Regional analysis confirmed the main effect of the task with significant BOLD signal increases in regions predicted to be activated by food rewards (**Figure 3**). Whole brain mapping demonstrated widespread activation involving these ROIs (as well as some other

cortical and subcortical regions) thus further justifying their prior selection (**Figure 3** and **SI Table S4** for anatomical details).

We tested for modulation of food reward-related activation by each drug in each ROI. A significant treatment effect was found only for GSK1521498 and only in the amygdala ($t = -5.9$, $df=8$, $P=0.0004$) (**Figure 3** and **SI Table S2**). GSK1521498 attenuated amygdalar activation in response to palatable stimuli; this effect remained after covarying for between-subject differences in baseline BOLD activation and opioid RO ($t = -3.1$, $df=12$, $P=0.0085$) (**SI Table S3**). The standardised effect size of GSK1521498 on amygdalar activation (-2.0; 95% CI -2.7 to -1.2) was greater than the corresponding effect size of NTX (-0.1; 95% CI -0.9 to 0.7); although the difference in effect sizes (0.6) was not quite significantly different from zero (95% CI, -0.04 to 1.3; $P=0.062$; see **SI Tables S2, S3** for details).

Whole brain mapping demonstrated attenuation of food reward-related activation by GSK1521498 in bilateral amygdala and ventral striatum, as well as thalamus and lateral cortical regions (**Figure 4** and **SI Table S4** for anatomical details). A similar analysis suggested that different anatomical regions (including the insula and dorsal striatum) were modulated by NTX (**Figure 4** and **SI Table S4** for anatomical details). A direct comparison between drugs showed that attenuation of food-related activation by GSK1521498 was greater than the effects of NTX in amygdala and ventral striatum bilaterally, whereas effects of NTX were greater than those of GSK1521498 primarily in the insula (**Figure 4** and **SI Table S4**).

DISCUSSION

We have combined molecular (PET) and functional (fMRI) neuroimaging techniques in an innovative experimental medicine study comparing the human pharmacology of two opioid receptor antagonists, NTX and GSK1521498. We have differentiated the two molecules based on both tissue PK and PD parameters. We propose that this general approach to integrated neuroimaging may provide a powerful new strategy for early evaluation of the therapeutic potential of new molecules.

Receptor occupancy

Both drugs dose dependently reduced the specific binding of [¹¹C]-carfentanil. GSK1521498 demonstrated high affinity for the target, and the relationship between its plasma concentration and μ -OR occupancy was time-independent. This allowed a simple direct relationship to be defined between plasma concentration and μ -OR binding for GSK1521498, distinguishing it from naltrexone, which demonstrated an indirect relationship between exposure and occupancy^{44, 45}. The indirect binding relationship observed for naltrexone could have several explanations. An oral dose of NTX undergoes rapid and extensive metabolism in humans, producing pharmacologically active metabolites, 6- β -NTX being the predominant one. Based on the plasma PK and in vitro receptor affinities of 6- β -NTX (**Table 1, SI Figure S1**), it seems likely that a substantial proportion of the target occupancy following an oral dose of NTX represents binding by 6- β -NTX. However, we have modelled the relationship between 6- β -NTX plasma concentration and RO over time, and found that this also exhibited an indirect relationship. We cannot exclude the presence of other active metabolites with a

different plasma kinetic profile from NTX, which could account for the observed RO time course. Alternatively, NTX or 6- β -NTX may have long residence times at the μ -OR, or either molecule may not diffuse passively across the blood-brain barrier or may be compartmentalized in the brain parenchyma. Any of these phenomena could result in slow equilibration between the μ -OR and the plasma compartments.

Functional efficacy

The pharmacological fMRI data indicated that GSK1521498 and NTX modulate different brain regions showing significant fMRI activation responses to palatable food stimuli. We did not find a significant effect of NTX in any of the pre-specified ROIs, whereas GSK1521498 was associated with significant attenuation of food-related activation in the amygdala. Whole brain mapping showed that effects of GSK1521498 were significantly greater on activation in the amygdala and ventral striatum, while any effects of NTX were greatest in the insular region. Previous fMRI studies have shown that BOLD activation in the amygdala and ventral striatum can be related to incentive salience and to behaviours reinforced by food or other rewards³⁵. The functional role of the insula is more complex, but it is known to play a role in interoceptive and gustatory processing^{46, 47}

Multiple factors could be responsible for pharmacodynamic differences between GSK1521498 and NTX. GSK1521498 has considerably greater selectivity for the μ -OR over the κ -OR than either NTX or 6- β -NTX (**Table 1**). Pre-clinical studies have indicated that κ -OR and μ -OR signalling may have different effects on feeding^{48, 49} and reward. Agonism at

μ -ORs facilitates dopaminergic neurotransmission in the ventral striatum, which has been specifically implicated in food reward processing. On the other hand, κ -OR agonism tends to reduce dopamine release in the ventral striatum^{50 51}. The reported selectivity of NTX and 6- β -NTX (**Table 1**) implies κ -OR occupancy in the range of 50-80% at doses which produce 80-90% occupancy of the μ -OR, making interactions between the two receptor systems relevant for the mode of action of NTX. It may also be relevant that GSK1521498, like NTX, can behave as a neutral antagonist or inverse agonist, depending on levels of constitutive activity, whereas 6- β -NTX behaves consistently as a neutral antagonist^{52 53}.

Methodological issues

A key strength of the study design is that the PET and fMRI data were acquired from the same participants in the same scanning sessions. This imposed the constraint that the first fMRI scan was always acquired pre-dose and the second scan was acquired post-dose, allowing the potential for task repetition effects on Δ -BOLD to confound effects of drug treatment. Post-hoc analysis of the regional fMRI data demonstrated that greater Δ -BOLD was often associated with greater baseline activation (**SI Figure S2**). Thus we cannot entirely exclude the possibility that the treatment difference in fMRI markers may be partly attributable to the interaction between a scanning order effect and sampling variation in baseline activation. However, the effect of GSK1521498 on amygdala activation remains significant after controlling for individual differences in baseline activation.

We chose to activate food reward systems directly by oral administration of a palatable stimulus, rather than by visual presentation of food images, to strengthen the translational link from the experimental data to potentially therapeutic effects of GSK1521498 on food consumption. Because of the radiation risks and costs of PET, the sample size was modest and conferred limited statistical power to detect treatment effects on fMRI measures. Finally, the sample comprised exclusively adult males with normal body weight, BMI and eating behaviours. Opioid receptor signalling may differ between sexes, and in relation to obesity and eating behaviours⁵⁴, so our results should be generalised judiciously.

Therapeutic implications

Drugs that attenuate μ -OR signalling are theoretically likely to be beneficial across a range of disorders of compulsive consumption, marked by habitual or uncontrollable ingestion of food, alcohol, opiates or stimulant drugs²⁷. The novel ligand GSK1521498 has high selectivity for the μ -OR *in vitro* and high affinity for opioid receptors *in vivo*. Compared to NTX, we have shown that it has a direct relationship between μ -OR occupancy and plasma concentration, and clearer evidence for functional efficacy in attenuating amygdala activation by food rewards. We hypothesise that these pharmacological differences may be associated with differences in therapeutic efficacy. For example, GSK1521498 may have greater efficacy than naltrexone in the treatment of maladaptive reward-driven eating behaviours, such as bingeing on energy-dense foods, that are commonly associated with obesity.

ACKNOWLEDGEMENTS

We thank the study participants, the staff of the GSK Clinical Imaging Centre, London, UK and the staff of Hammersmith Medicines Research, for their support in conduct of the study; Wenli Tao and David Collins for statistical advice on study design; and members of the GSK1521498 project team.

CONFLICT OF INTEREST

All the authors are full-time or part-time employees and share-holders of GlaxoSmithKline (GSK). GSK has a commercial interest in GSK1521498 and was the sponsor of this study.

REFERENCES

1. Lord JAH, Waterfield AA, Hughes J, and Kosterlitz HW. Endogenous opioid peptides: multiple agonists and receptors. *Nature* 1977. **267**: 495-499.
2. Mansour A, Hoversten MT, Taylor LP, Watson SJ, and Akil H. The cloned m, d and k receptors and their endogenous ligands: Evidence for two opioid peptide recognition cores. *Brain Research* 1995. **700**: 89-98.
3. Snyder SH and Pasternak GW. Historical review: Opioid receptors. *Trends in Pharmacological Sciences* 2003. **24**: 198-205.
4. Leibowitz SF. Brain neurotransmitters and appetite regulation. *Psychopharmacology Bulletin* 1985. **21**: 412-418.
5. Morley JE. Neuropeptide regulation of appetite and weight. *Endocrine Reviews* 1987. **8**: 256-287.
6. Cooper S and Kirkham T. Opioid mechanisms in the control of food consumption and taste preferences. Opioids II, in A. Herz, Editor *Handbook of experimental pharmacology*. 1993, Springer-Verlag: Berlin pp. 239- 62.
7. Gosnell B and Levine A. Stimulation of ingestive behavior by preferential and selective opioid agonists. Drug receptor subtypes and ingestive behavior. 1996, Academic Press. pp. 147- 66.
8. Glass MJ, Billington CJ, and Levine AS. Opioids and food intake: Distributed functional neural pathways? *Neuropeptides* 1999. **33**: 360-368.
9. Nathan PJ and Bullmore ET. From taste hedonics to motivational drive: Central - opioid receptors and binge-eating behaviour. *International Journal of Neuropsychopharmacology* 2009. **12**: 995-1008.
10. Gosnell BA, Levine AS, and Morley JE. The stimulation of food intake by selective agonists of mu, kappa and delta opioid receptors. *Life Sciences* 1986. **38**: 1081-1088.
11. Bakshi VP and Kelley AE. Feeding induced by opioid stimulation of the ventral striatum: Role of opiate receptor subtypes. *Journal of Pharmacology and Experimental Therapeutics* 1993. **265**: 1253-1260.
12. Shippenberg TS and Elmer GI. The neurobiology of opiate reinforcement. *Critical Reviews in Neurobiology* 1998. **12**: 267-303.
13. Kelley AE, Bakshi VP, Haber SN, Steininger TL, Will MJ, and Zhang M. Opioid modulation of taste hedonics within the ventral striatum. *Physiology and Behavior* 2002. **76**: 365-377.
14. Figlewicz DP and Sipols AJ. Energy regulatory signals and food reward. *Pharmacology Biochemistry and Behavior* 2010. **97**: 15-24.
15. Peciña S and Berridge KC. Hedonic hot spot in nucleus accumbens shell: Where do μ -Opioids cause increased hedonic impact of sweetness? *Journal of Neuroscience* 2005. **25**: 11777-11786.
16. Zhang M and Kelley AE. Opiate agonists microinjected into the nucleus accumbens enhance sucrose drinking in rats. *Psychopharmacology* 1997. **132**: 350-360.
17. Wright CI, Beijer AVJ, and Groenewegen HJ. Basal amygdaloid complex afferents to the rat nucleus accumbens are compartmentally organized. *Journal of Neuroscience* 1996. **16**: 1877-1893.
18. Azuma S, Yamamoto T, and Kawamura Y. Studies on gustatory responses of amygdaloid neurons in rats. *Experimental Brain Research* 1984. **56**: 12-22.
19. Yamamoto T, Shimura T, Sako N, Yasoshima Y, and Sakai N. Neural substrates for conditioned taste aversion in the rat. *Behavioural Brain Research* 1994. **65**: 123-137.
20. Cardinal RN, Parkinson JA, Hall J, and Everitt BJ. Emotion and motivation: The role of the amygdala, ventral striatum, and prefrontal cortex. *Neuroscience and Biobehavioral Reviews* 2002. **26**: 321-352.
21. Kelley AE, Schiltz CA, and Landry CF. Neural systems recruited by drug- and food-related cues: Studies of gene activation in corticolimbic regions. *Physiology and Behavior* 2005. **86**: 11-14.
22. Will MJ, Franzblau EB, and Kelley AE. The amygdala is critical for opioid-mediated

- binge eating of fat. *NeuroReport* 2004. **15**: 1857-1860.
23. Yeomans MR and Gray RW. Opioid peptides and the control of human ingestive behaviour. *Neuroscience and Biobehavioral Reviews* 2002. **26**: 713-728.
 24. Fantino M, Hosotte J, and Apfelbaum M. An opioid antagonist, naltrexone, reduces preference for sucrose in humans. *American Journal of Physiology - Regulatory Integrative and Comparative Physiology* 1986. **251**.
 25. Yeomans MR and Wright P. Lower pleasantness of palatable foods in nalmefene-treated human volunteers. *Appetite* 1991. **16**: 249-259.
 26. Yeomans MR. Palatability and the micro-structure of feeding in humans: The appetizer effect. *Appetite* 1996. **27**: 119-133.
 27. Drewnowski A, Krahn DD, Demitrack MA, Nairn K, and Gosnell BA. Naloxone, an opiate blocker, reduces the consumption of sweet high-fat foods in obese and lean female binge eaters. *American Journal of Clinical Nutrition* 1995. **61**: 1206-1212.
 28. Drewnowski A, Krahn DD, Demitrack MA, Nairn K, and Gosnell BA. Taste responses and preferences for sweet high-fat foods: Evidence for opioid involvement. *Physiology and Behavior* 1992. **51**: 371-379.
 29. Nathan P, O'Neill B, Bush M, Koch A, Tao W, Maltby K, et al. Opioid receptor modulation of hedonic taste preference and food intake: A single dose safety, pharmacokinetic and pharmacodynamic investigation with GSK1521498, a novel mu opioid receptor inverse agonist. *Journal of Clinical Pharmacology (in press)*.
 30. O'Doherty JP, Deichmann R, Critchley HD, and Dolan RJ. Neural responses during anticipation of a primary taste reward. *Neuron* 2002. **33**: 815-826.
 31. Filbey FM, Claus E, Audette AR, Niculescu M, Banich MT, Tanabe J, et al. Exposure to the taste of alcohol elicits activation of the mesocorticolimbic neurocircuitry. *Neuropsychopharmacology* 2008. **33**: 1391-1401.
 32. Stice E, Spoor S, Bohon C, Veldhuizen MG, and Small DM. Relation of Reward From Food Intake and Anticipated Food Intake to Obesity: A Functional Magnetic Resonance Imaging Study. *Journal of Abnormal Psychology* 2008. **117**: 924-935.
 33. Petrovic P, Pleger B, Seymour B, Klöppel S, De Martino B, Critchley H, et al. Blocking central opiate function modulates hedonic impact and anterior cingulate response to rewards and losses. *Journal of Neuroscience* 2008. **28**: 10509-10516.
 34. Myrick H, Anton RF, Li X, Henderson S, Randall PK, and Voronin K. Effect of naltrexone and ondansetron on alcohol cue-induced activation of the ventral striatum in alcohol-dependent people. *Archives of General Psychiatry* 2008. **65**: 466-475.
 35. Fletcher PC, Napolitano A, Skeggs A, Miller SR, Delafont B, Cambridge VC, et al. Distinct modulatory effects of satiety and sibutramine on brain responses to food images in humans: A double dissociation across hypothalamus, amygdala, and ventral striatum. *Journal of Neuroscience* 2010. **30**: 14346-14355.
 36. In British National Formulary, 59. . 2010: Royal Pharmaceutical Society.
 37. Jewett DM. A simple synthesis of [¹¹C]carfentanil using an extraction disk instead of HPLC. *Nuclear Medicine and Biology* 2001. **28**: 733-734.
 38. Tziortzi AC, Searle GE, Tzimopoulou S, Salinas C, Beaver JD, Jenkinson M, et al. Imaging dopamine receptors in humans with [¹¹C]-(+)-PHNO: Dissection of D3 signal and anatomy. *NeuroImage* 2010. **54**: 264-277.
 39. Innis RB, Cunningham VJ, Delforge J, Fujita M, Gjedde A, Gunn RN, et al. Consensus nomenclature for in vivo imaging of reversibly binding radioligands. *J Cereb Blood Flow Metab* 2007. **27**: 1533-9.
 40. Gunn RN, Lammertsma AA, Hume SP, and Cunningham VJ. Parametric imaging of ligand-receptor binding in PET using a simplified reference region model. *Neuroimage* 1997. **6**: 279-87.
 41. Jack Jr CR, Bernstein MA, Fox NC, Thompson P, Alexander G, Harvey D, et al. The Alzheimer's Disease Neuroimaging Initiative (ADNI): MRI methods. *Journal of Magnetic Resonance Imaging* 2008. **27**: 685-691.
 42. Karlsson J, Persson LO, Sjöström L, and Sullivan M. Psychometric properties and factor structure of the Three-Factor Eating Questionnaire (TFEQ) in obese men and women. Results from the Swedish Obese Subjects (SOS) study. *International Journal*

- of Obesity* 2000. **24**: 1715-1725.
43. Patton JH, Stanford MS, and Barratt ES. Factor structure of the Barratt Impulsiveness Scale. *Journal of Clinical Psychology* 1995. **51**: 768-774.
 44. Abanades S, van der Aart J, Barletta JA, Marzano C, Searle GE, Salinas CA, et al. Prediction of repeat-dose occupancy from single-dose data: characterisation of the relationship between plasma pharmacokinetics and brain target occupancy. *Journal of Cerebral Blood Flow and Metabolism (in press)*.
 45. Derendorf H and Meibohm B. Modeling of pharmacokinetic/pharmacodynamic (PK/PD) relationships: Concepts and perspectives. *Pharmaceutical Research* 1999. **16**: 176-185.
 46. Small DM. Taste representation in the human insula. *Brain Structure and Function (in press)* 1-11.
 47. Small DM and Prescott J. Odor/taste integration and the perception of flavor. *Experimental Brain Research* 2005. **166**: 345-357.
 48. Wolinsky TD, Carr KD, Hiller JM, and Simon EJ. Effects of chronic food restriction on mu and kappa opioid binding in rat forebrain: A quantitative autoradiographic study. *Brain Research* 1994. **656**: 274-280.
 49. Wolinsky TD, Carr KD, Hiller JM, and Simon EJ. Chronic food restriction alters μ and κ opioid receptor binding in the parabrachial nucleus of the rat: A quantitative autoradiographic study. *Brain Research* 1996. **706**: 333-336.
 50. Buijnzeel AW. kappa-Opioid receptor signaling and brain reward function. *Brain Research Reviews* 2009. **62**: 127-146.
 51. Shippenberg TS, Zapata A, and Chefer VI. Dynorphin and the pathophysiology of drug addiction. *Pharmacology and Therapeutics* 2007. **116**: 306-321.
 52. Raehal KM, Lowery JJ, Bhamidipati CM, Paolino RM, Blair JR, Wang D, et al. In vivo characterization of 6 β -naltrexol, an opioid ligand with less inverse agonist activity compared with naltrexone and naloxone in opioid-dependent mice. *Journal of Pharmacology and Experimental Therapeutics* 2005. **313**: 1150-1162.
 53. Wang D, Sun X, and Sadee W. Different effects of opioid antagonists on μ -, δ -, and κ -opioid receptors with and without agonist pretreatment. *Journal of Pharmacology and Experimental Therapeutics* 2007. **321**: 544-552.
 54. Bencherif B, Guarda AS, Colantuoni C, Ravert HT, Dannals RF, and Frost JJ. Regional μ -opioid receptor binding in insular cortex is decreased in bulimia nervosa and correlates inversely with fasting behavior. *Journal of Nuclear Medicine* 2005. **46**: 1349-1351.
 55. Pelotte AL, Smith RM, Ayestas M, Dersch CM, Bilsky EJ, Rothman RB, et al. Design, synthesis, and characterization of 6 β -naltrexol analogs, and their selectivity for in vitro opioid receptor subtypes. *Bioorganic and Medicinal Chemistry Letters* 2009. **19**: 2811-2814.
 56. Ko MCH, Divin MF, Lee H, Woods JH, and Traynor JR. Differential in vivo potencies of naltrexone and 6 β -naltrexol in the monkey. *Journal of Pharmacology and Experimental Therapeutics* 2006. **316**: 772-779.
 57. Meyer MC, Straughn AB, and Lo MW. Bioequivalence, dose-proportionality, and pharmacokinetics of naltrexone after oral administration. *Journal of Clinical Psychiatry* 1984. **45**: 15-19.
 58. Beck AT, Steer RA, and Brown GK, In Manual for Beck Depression Inventory - II. 1996, San Antonio, Texas: Psychological Corporation.
 59. Schutz HG and Cardello AV. A labeled affective magnitude (LAM) scale for assessing food liking/disliking. *Journal of Sensory Studies* 2001. **16**: 117-159.

TABLES

Table 1: Opioid receptor subtype binding affinities and plasma pharmacokinetic parameters for naltrexone (NTX), 6- β -naltrexol (6- β -NTX) and GSK1521498.

| Opioid receptor subtype affinity (nM) | | | |
|--|-------------------------|---------------------------------------|-------------------|
| | Naltrexone | 6-β-naltrexol | GSK1521498 |
| μ -OR | 0.5 ⁵³ | 1.4 ⁵³ | |
| | | 2.1 ⁵⁵ | |
| | 0.31 ⁵⁶ | 0.74 ⁵⁶ | |
| | 4.7 * | | 1.5 * |
| κ -OR | 1.0⁵³ | 2.0⁵³ | |
| | | 7.4 ⁵⁵ | |
| | 20.0 * | | 20.4 * |
| δ -OR | 7.0 ⁵³ | 29 ⁵³ | |
| | | 213 ⁵⁵ | |
| | 42 * | | 30.2 * |
| Pharmacokinetic parameters (minimum-maximum) | | | |
| AUC(0, t), ng*h/mL | 0.06 - 23.6 | 14.1 – 618 | 20.4 – 10 422 |

| | | | |
|--------------------------------------|-----------------|------------------|---------------------|
| AUC(0, t), nM*h | 0.18 - 69.1 | 41 – 1 800 | 50.7 – 25 842 |
| Cmax, ng/mL | 0.046 - 9.01 | 1.2 – 93 | 1.5 – 929 |
| Cmax, nM | 0.13 - 26.4 | 3.5 - 271 | 3.8 - 2308 |
| Exposures during PET scanning, ng/mL | 0.013 - 1.87 | 0.32 - 37.8 | 1.1 – 286 |
| Exposures during PET scanning, nM | 0.04 - 5.5 | 0.94 - 110 | 2.7 - 711 |
| Tmax, h | 0.5-2 | 0.5-2 | 1-4 |
| T 1/2, h | 4 ⁵⁷ | 13 ⁵⁷ | 20-24 ²⁹ |

* GSK internal data.

Table notes: While data from different studies can be used to compare drug selectivities at the OR subtypes, comparison of absolute affinity values from different studies should be done cautiously due to differences in the system examined and assay conditions. Affinity data was estimated from pKi of displacement of appropriate radioligands from human ORs expressed in a cell system^{53, 55}, or from monkey cortical homogenates⁵⁶. The GSK internal data were estimated from a functional (f)pKi in a [³⁵S]GTPγS assay on human OR expressed in CHO-E1A cells.

FIGURES

Figure 1: Opioid receptor binding by [¹¹C]-carfentanil and its displacement by naltrexone and GSK1521498. (a) Slices of an individual PET scan demonstrating high binding in subcortical nuclei at baseline which was reduced following administration of GSK1521498 50mg. (b) Time-activity curves for ventral striatum (VST, red lines) and for occipital cortex (black lines) at baseline (solid lines) and after a dose of GSK1521498 50mg (broken lines). Dose-occupancy curves for (c) GSK1521498 and (d) NTX, estimated from scans acquired < 8 h after dosing. Vertical line indicates ED₅₀ and the dotted lines are its 95% CI.

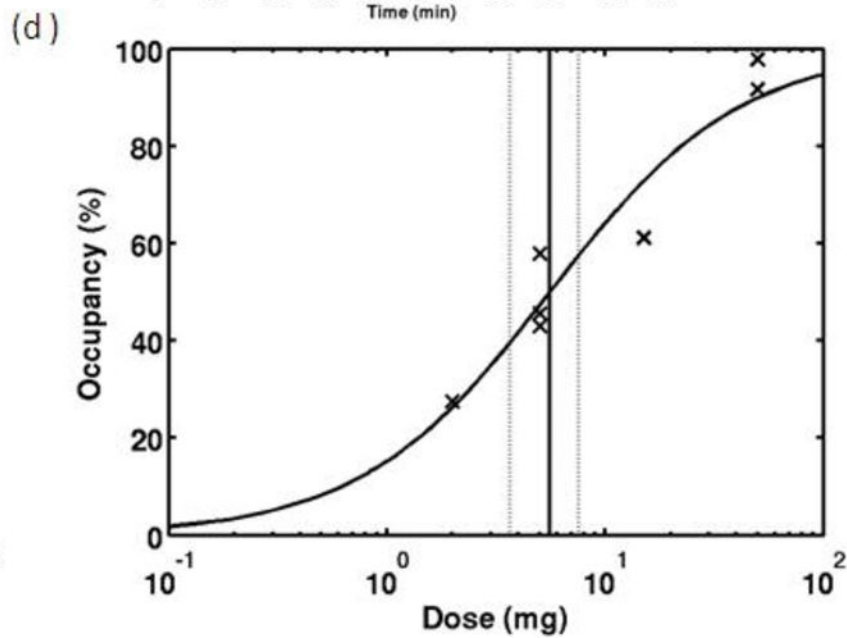
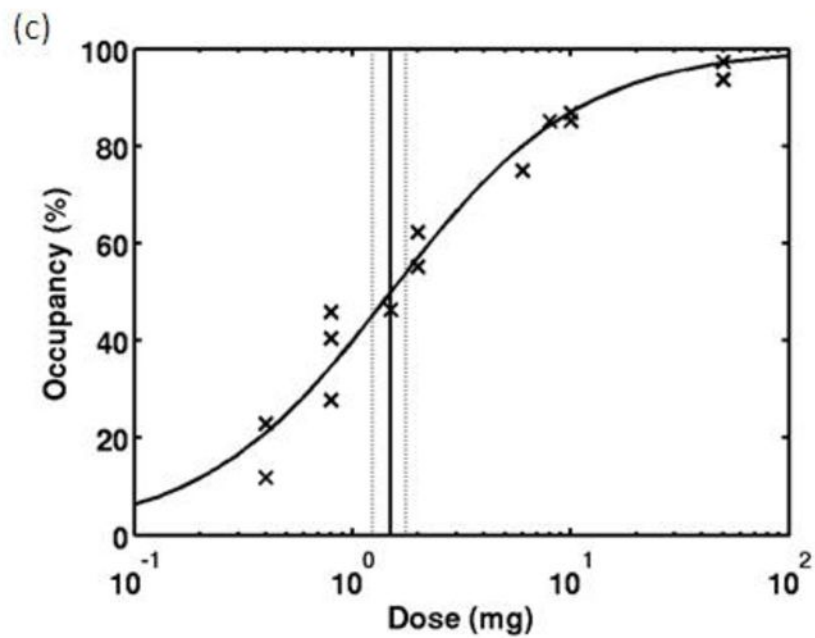
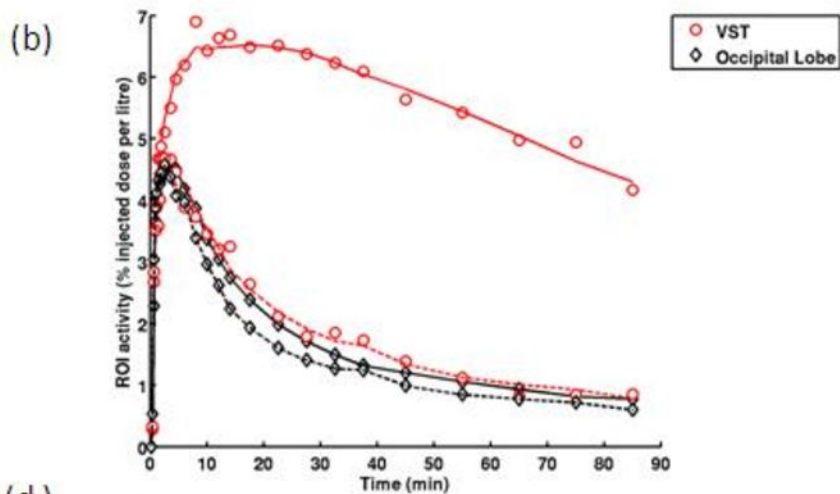
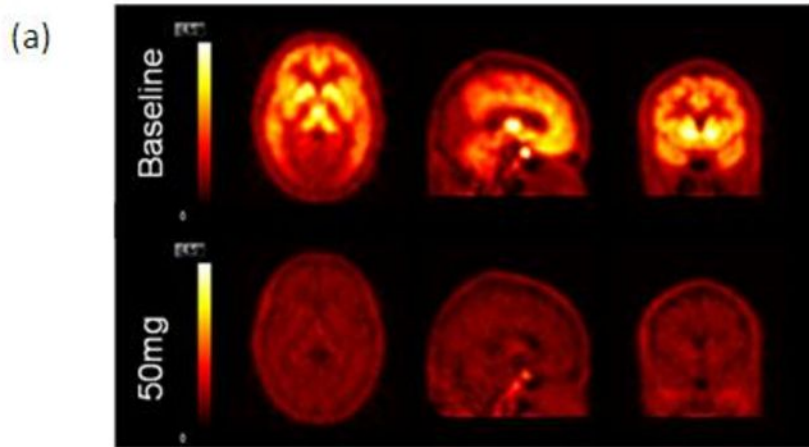
Figure 2: Relationships between plasma concentration and opioid receptor occupancy for (a) GSK1521498, (b) naltrexone, and (c) 6-β-naltrexol. The timing of individual scans after administration of GSK1521498 or naltrexone is indicated by the shape of the point markers. For GSK1521498, the relationship between plasma exposure and RO is independent of time and well fitted by Eq 3; the vertical line indicates the EC₅₀ and the dotted lines its 95% CI. For NTX and 6-β-NTX, at a given plasma concentration, RO is greater for later scans; this hysteresis is highlighted by the arrow which indicates the time ordering of scans.

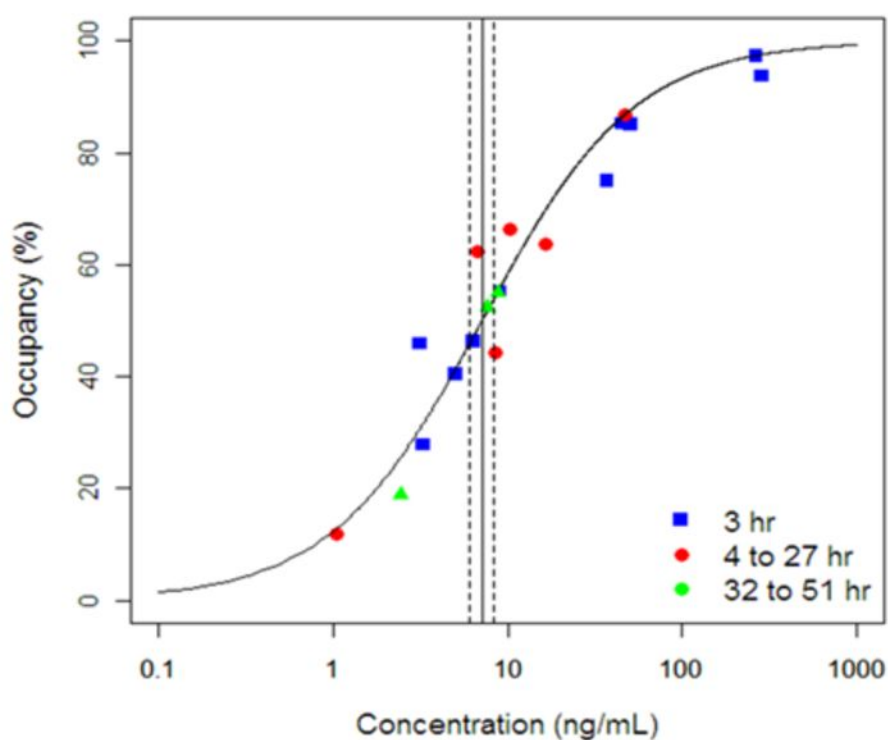
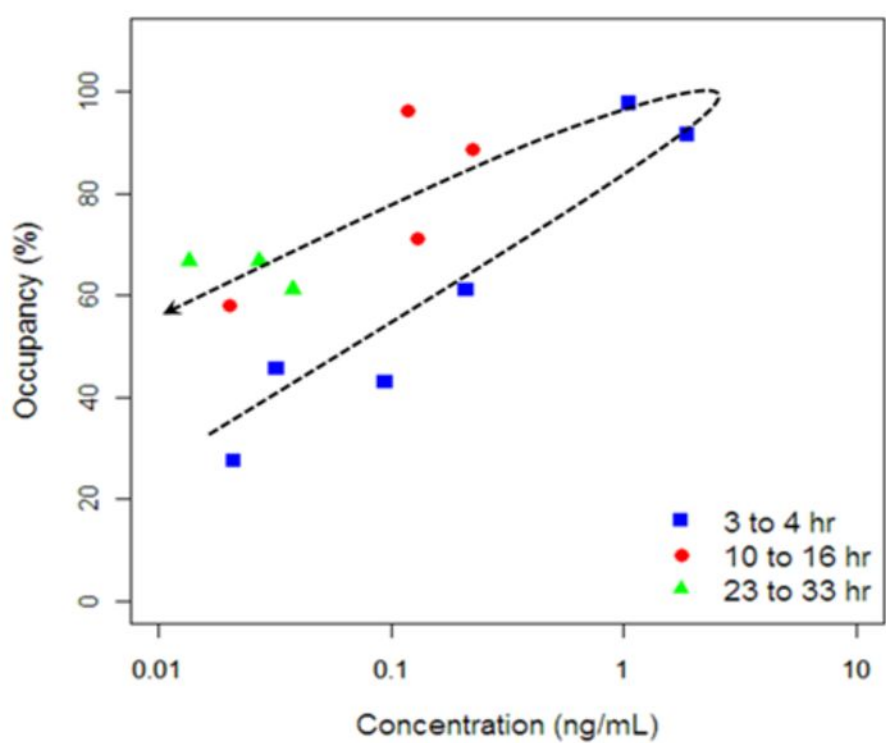
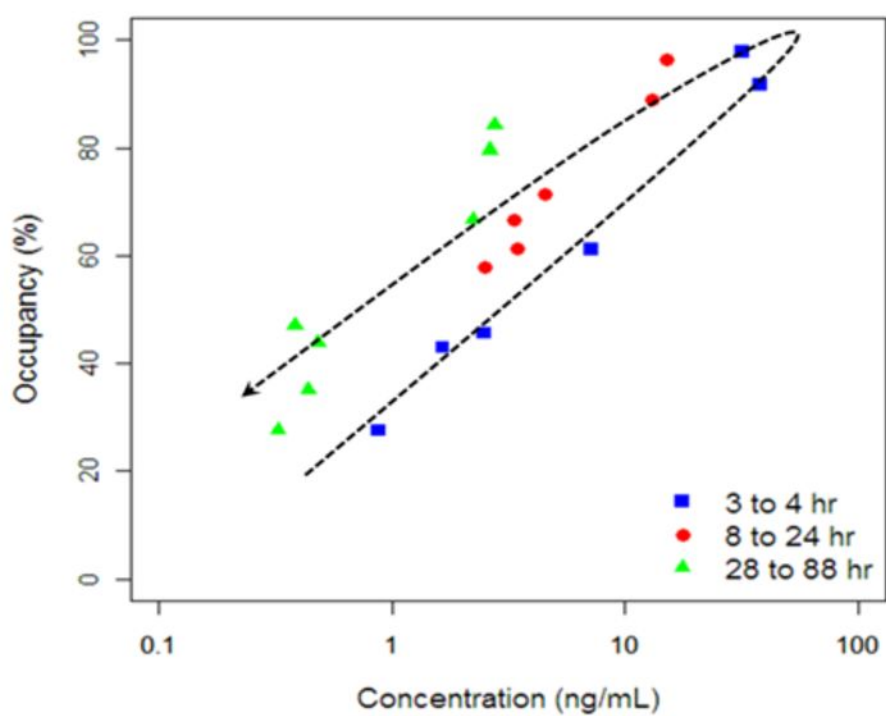
Figure 3: Brain activation by a palatable food stimulus and the effects of GSK1521498 and naltrexone on food reward-related activation in selected regions of interest. (a)

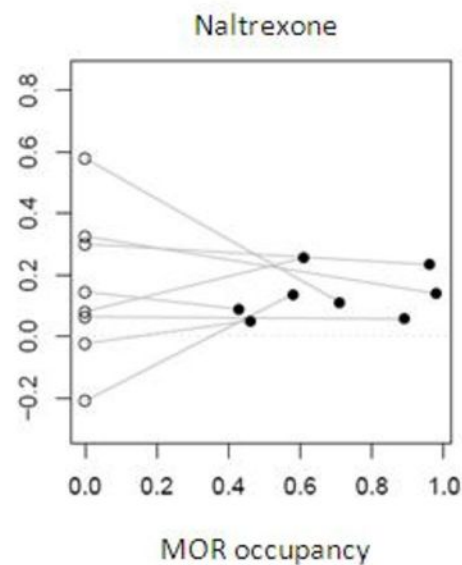
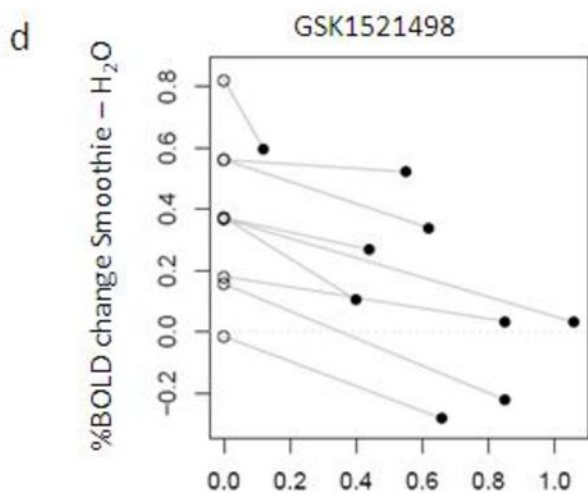
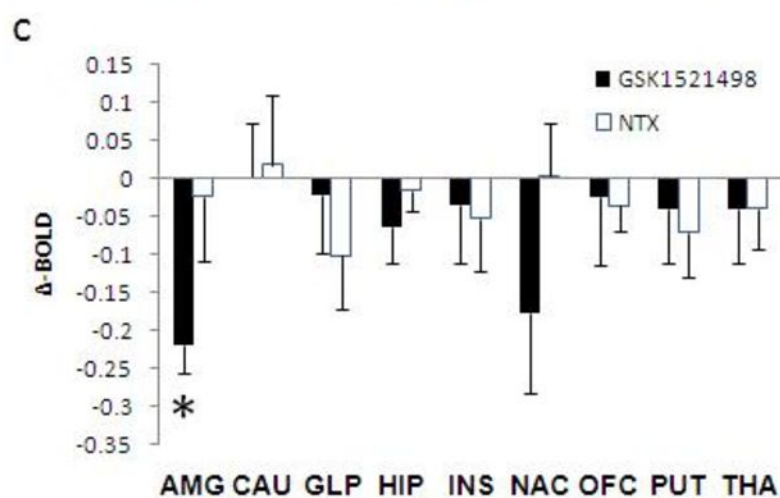
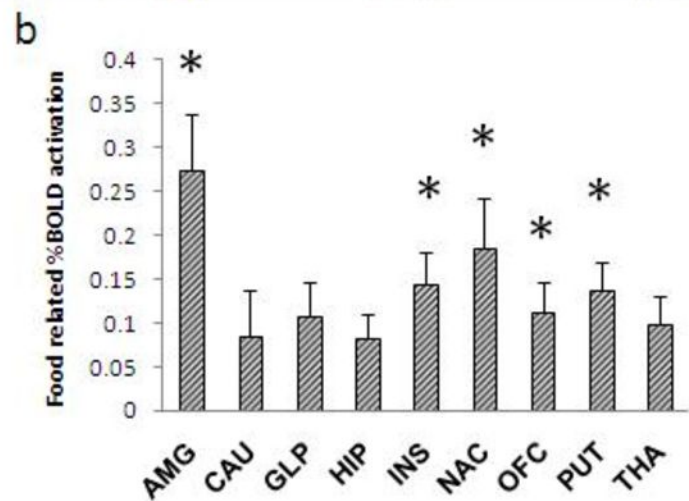
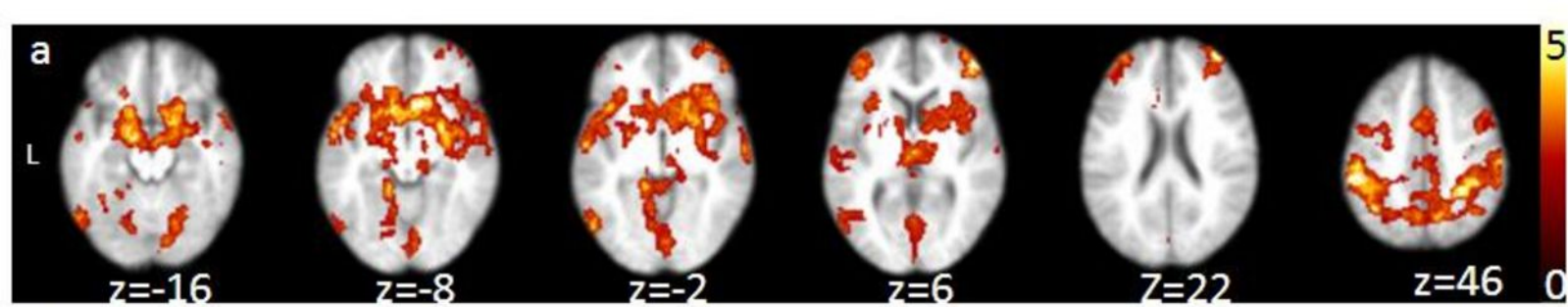
Whole brain map of brain regions activated by experimental contrast between palatable food stimulus and purified water; z indicates distance (mm) superior or inferior to the inter-

commissural plane in standard stereotactic space. (b) Bar chart showing magnitude of BOLD activation by palatable stimuli vs purified water in 9 pre-specified ROIs: amygdala (AMG), caudate (CAU), globus pallidus (GLP), hippocampus (HIP), insula (INS), nucleus accumbens (NAC), orbitofrontal cortex (OFC), putamen (PUT), and thalamus (THA). (c) Bar chart showing magnitude of change in food-related activation, Δ -BOLD, following treatment with GSK1521498 or naltrexone (NTX) in the same 9 ROIs. (d) Plots of BOLD activation by palatable stimuli vs RO from pre- and post-dose scans for each participant in each of the treatment groups. Asterisks (*) denote effects that are significantly different from zero at $P < 0.05$ (Bonferroni corrected).

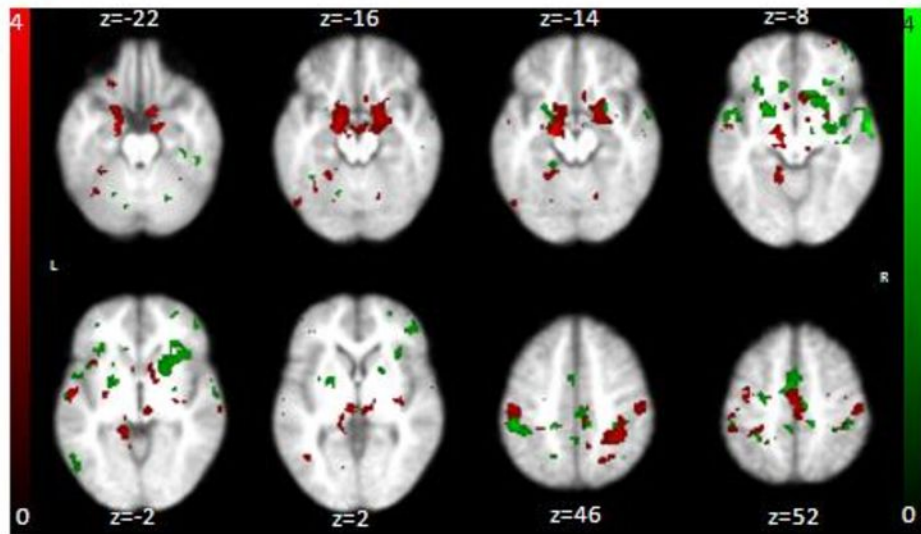
Figure 4: Whole brain mapping of treatment-related decreases in brain activation by food rewards. (a) Maps of significant Δ -BOLD change in the NTX-treated group (green voxels) or in the GSK1521498-treated group (red voxels). (b) Map of significant differences in Δ -BOLD between treatment groups: Δ -BOLD_{GSK1521498} > Δ -BOLD_{NTX} (yellow voxels) or Δ -BOLD_{NTX} > Δ -BOLD_{GSK1521498} (green voxels). Z indicates distance (mm) superior or inferior to the inter-commissural plane in standard stereotactic space



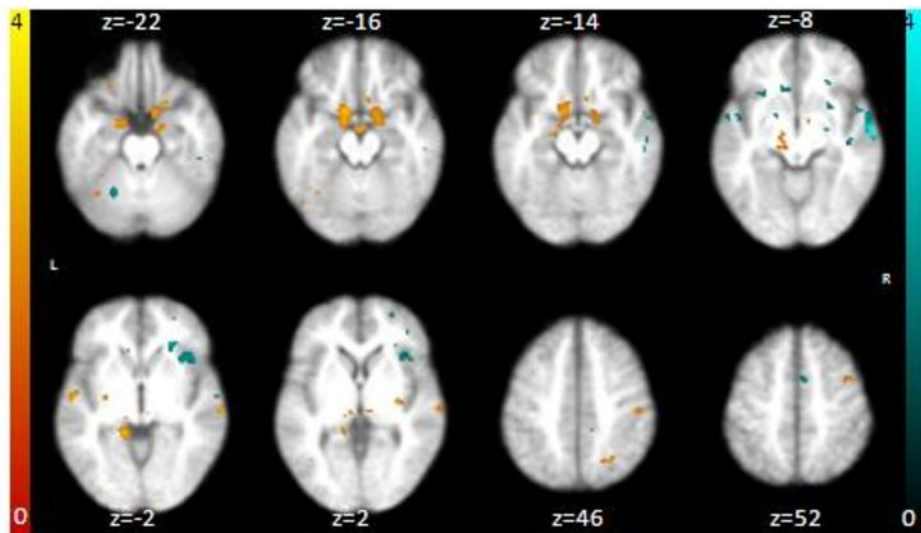
(a)**(b)****(c)**



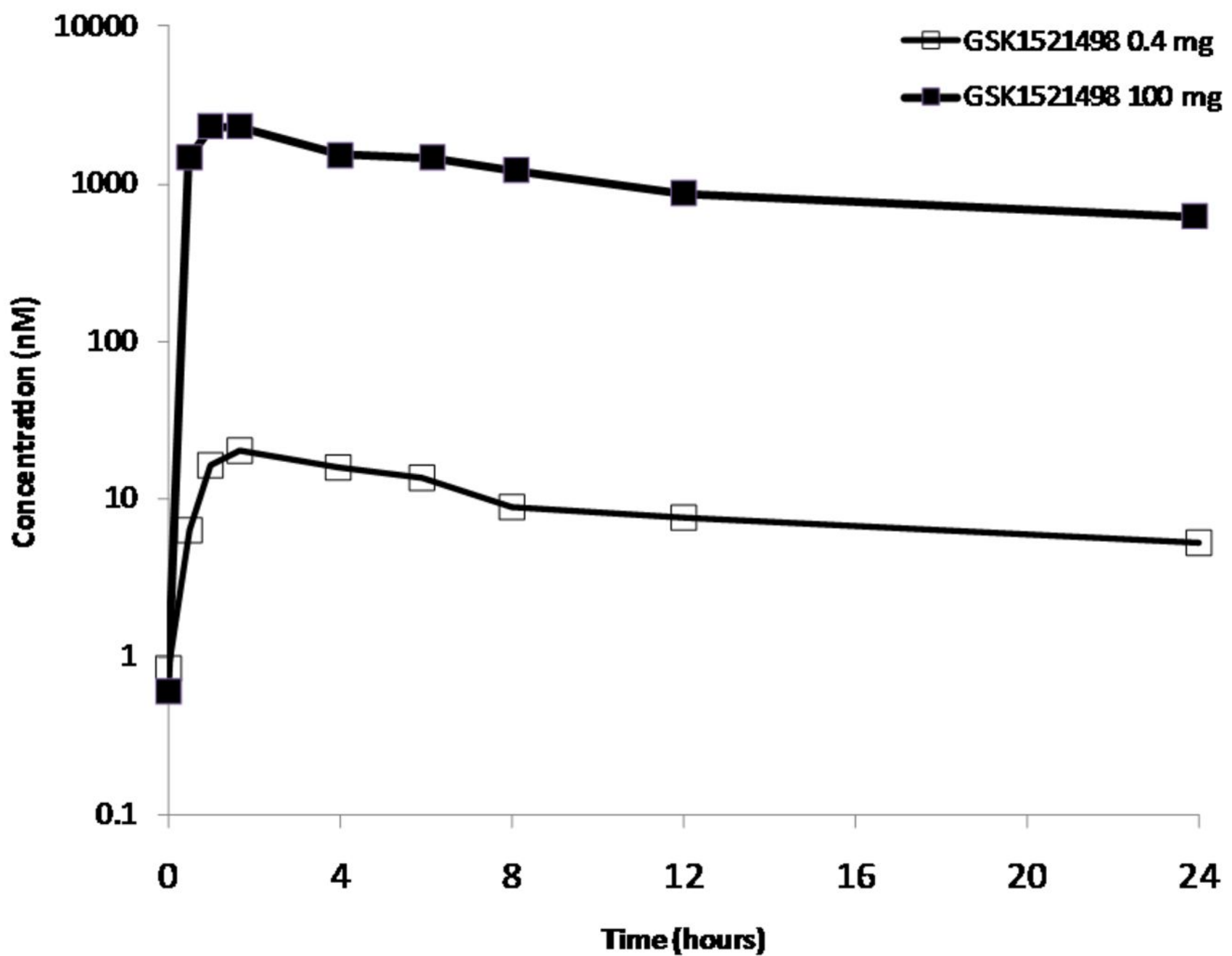
A



B



(a)



(b)

